Energy-Efficient Cooperative Resource Allocation in Wireless Powered Mobile Edge Computing

Luyue Ji and Songtao Guo

***Abstract*—Mobile edge computing (MEC) as an emerging and prospective computing paradigm, offloads the computation-intensive tasks from resources-constrained smart mobile devices (SMDs) to edge cloud or server so as to enhance computation capability of SMDs. Meanwhile, it is expected that wireless power transfer (WPT) is applied to MEC (WPT-MEC) in order to prolong operation time of the battery. However, how to achieve the energy-effective computation offloading in WPT-MEC system under the hard constraint remains a challenge issue. To address this challenge, this paper considers energy-effective resource allocation policy in a two-user WPT-MEC system. We first formulate the maximization minimum energy efficiency (EE) problem to ensure the fairness of users. Then, due to the "doubly near–far" problem, we propose a user cooperative scheme in which the near user can forward the far user's tasks to the edge cloud utilizing its more harvested energy. Considering the green network, we attach the scheme to maximize the users' EE, defined as a ratio of the user throughput to its harvested or consumptive energy, subject to the constraints of the computational tasks in two schemes. We convert two problems into their equivalent parameterized subtractive form and provide the corresponding optimal solutions via two efficient optimization algorithms. Numerical results show that the optimal WPT-MEC system with cooperation has significant performance enhancement over the systems without cooperation.**

***Index Terms*—Doubly near–far problem, energy efficiency maximization, mobile edge computing (MEC), user cooperation, wireless power transfer (WPT).**

I. Introduction

THE RAPID development of Internet of Things (IoT) has drastically increased the number of computationally intensive mobile applications including autonomous driving, virtual reality, interactive online games, etc., [1]. In order to support resource-constrained (computation, storage, and battery capacity) mobile devices (MDs), mobile edge computing (MEC) as a promising computation paradigm has received extensive attentions from academia and industry. MEC pushes cloud services down to the proximity of MDs located at the edge of network so as to shorten user service latency by offloading traffics to mobile edge devices. It is regarded as one of the key technologies for the fifth generation (5G) by the European 5G PPP (5G Infrastructure Public Private Partnership). Compared with mobile cloud computing, MEC has some obvious benefits, such as low latency, proximity, high bandwidth, real time radio network information, and location awareness. Through migrating the computation, storage, and servicing capability onto the edge of network, MEC makes applications, services, and contents be deployed locally with short distance in a distributed way. To a certain degree, it will satisfy the critical requirements of future enhanced mobile broadband, ultrareliable low latency communication, and massive machine type communication scenarios in 5G wireless systems [2].

The pressure of computation-intensive applications promotes the MDs with constrained resources to offload part or all of their computation-intensive latency-critical tasks to edge cloud with more resources. A novel resource allocation approach was proposed in [3] on both communication and computation resources-based augmented reality applications, which have inherent synergistic properties in terms of data collection in the uplink, computing at the edge, and data delivery in the downlink. Resource allocation in a multiuser MEC system was studied in [4], based on both time-division multiple access (TDMA) and orthogonal frequency-division multiple access. The energy-effective resource allocation schemes were considered in [5], for a multiuser MEC system with inelastic computation tasks and non-negligible task execution durations.

Beside the computation resource constraint, traditional IoT devices are restricted by limited battery capacity, which is taken as another performance bottleneck that IoT faces. It may be solved by using the batteries with large capacity or rechargeable batteries. However, the former causes more hardware cost while the latter may be impossible in certain application scenarios, e.g., in the wireless sensor networks and the IoT for surveillance where the nodes are typically hard-to-reach [6]. To overcome the bottleneck, energy harvesting (EH) [7] has emerged as a promising technology in MEC which used to be applied in wireless powered communication networks (WPCNs). EH can capture ambient recyclable energy, such as solar radiation, wind energy, and human motion energy [8], [9], and thus it facilitates self-sustainability and permanent operation [10], [11].

Manuscript received June 16, 2018; revised October 1, 2018; accepted October 29, 2018. Date of publication November 12, 2018; date of current version June 19, 2019. This work was supported in part by the National Key Research and Development Program of China under Grant 2018YFB0803400, in part by the National Natural Science Foundation of China under Grant 61772432 and Grant 61772433, in part by the Natural Science Key Foundation of Chongqing under Grant cstc2015jcyjBX0094, in part by the Fundamental Research Funds for the Central Universities under Grant XDJK2016A011, and in part by the Natural Science Foundation of Chongqing under Grant CSTC2016JCYJA0449. *(Corresponding author: Songtao Guo.)*

L. Ji is with the College of Electronic and Information Engineering, Southwest University, Chongqing 400715, China.

S. Guo is with the College of Computer Science, Chongqing University, Chongqing 400044, China, and also with the College of Electronic and Information Engineering, Southwest University, Chongqing 400715, China (e-mail: songtao_guo@163.com).

Digital Object Identifier 10.1109/JIOT.2018.2880812

Due to the intermittency and unpredictability of renewable sources, the energy harvested from the surrounding environment is dynamically changing with uncertain time and quantity, which makes it very challenging to deliver a high quality of service (QoS) to users in EH MEC systems. Thus, Zhao *et al.* proposed a unified framework to jointly study WPT and interference alignment (IA) and a power splitting optimization algorithm in [12], to simultaneously optimize both information transmission (IT) and WPT performance in IA networks. The average function, the probability density function, and the cumulative distribution function of the harvested power were studied in [13], where the channels are assumed to be Rician fading or Gamma-shadowed Rician fading.

Meanwhile, applying wireless power transfer (WPT) to energy-constrained MEC systems, which is called as wireless powered MEC systems, can prolong system lifetime via charging low-power devices with dedicated wireless signals even interference [14]. There are some existing studies on WPT-MEC systems [15]–[18]. Bi and Zhang [15] proposed a joint optimization method with binary offloading based on the alternating direction method of multipliers (ADMM) decomposition technique in a WPT-MEC network. Zhou *et al.* [16] studied the computation rate maximization problems in an unmanned aerial vehicle-enabled multiuser WPT-MEC system under both binary and partial computation offloading modes. Hu *et al.* [17] proposed wireless powered computation offloading scheme with user cooperation (UC-JOPT) by jointly optimizing power and time allocation. Dinh *et al.* [18] proposed an optimization framework of offloading (OPT-OFF) from a single MD to multiple edge devices, which aim to minimize both total tasks' execution latency and the MDs energy consumption by jointly optimizing the task allocation decision and the MD's central process unit (CPU) frequency.

Whereas, multiuser WPT-MEC systems are susceptible to suffer from the alleged "double-near–far" effect. In such networks, the users closer to access point or power bacon experience better channel conditions than further ones, which means that closer users usually possess better EH and information transfer. To overcome the effect, there are some existing technologies [19]–[22] applied to multiuser WPCNs such as beam forming and relay protocol (e.g., amplify-and-forward and decode-and-forward). Compared with beam forming, relay protocol is easy to implement in practice. Especially, Chen *et al.* [23] presented a pricing mechanism to incent the closer user to share its excess energy to help an further user complete its IT. A cooperative wireless-powered communication network protocol is proposed, in which user far away from a hybrid access point (HAP) is capable of harvesting wireless powers by overhearing the uplink signals of users that are relatively nearer to the HAP, in addition to downlink signal broadcast by the HAP [24].

In regard to EE of systems, Zhou *et al.* [25] focused on optimal computing manner by integrating collaboration with intelligence through computing the correlation coefficient, which links energy consumption with the content relationship of the transmitted data in general Industrial Internet of Things systems. Moreover, they proposed a systematic solution for content delivery over ultradense networks by integrating collaboration with intelligence through evaluating energy-spectrum efficiency index in [26].

Therefore, in this paper, we propose two different offloading schemes for solving two aforementioned problems, to complete the computation-intensive tasks of two near–far users,[1] where the entire process is powered by the HAP. In our first scheme two users are noncooperative and offload their tasks onto the edge cloud independently. We maximizes the individual energy efficiency (EE) of each user, defined as a ratio of the user throughput to its harvested energy, based on the max-min criterion. Utilizing cooperative communication, in our second scheme, the near user (NU) forwards the far user (FU)'s tasks to the edge cloud first as a relay node and then offloads its own tasks to maximize the total EE of the system.

Compared with some previous works on WPT-MEC system, such as UC-JOPT [17] and OPT-OFF [18], which paid attention to execution cost minimization (e.g., the execution latency, consumption energy, and task failure), our target is to maximize the system's EE in view of going green and environmental protection. In addition, unlike prior works on multiuser wireless powered MEC models, we establish a collaborative offloading mechanism to eliminate double-near–far effect with the relay protocol. Furthermore, unlike the way used in [25] and [26], we evaluate the high-performance through EE (i.e., the ratio of transmitted data to energy) by Dinkelbach's method [27] in the proposed WPE-MEC scheme. The main contributions of this paper are summarized as follows.

1) Our two different resource allocation schemes are based on the harvest-then-offload protocol with TDMA mechanism, which are more effective in energy-constrained system, exploiting cooperative communications to overcome the energy-constrained problem, and doubly near–far effect in two-user WPT-MEC system.
2) Specifically, the first scheme considers the fairness between two users while the second one pays attention to its system EE. Furthermore, we formulate an EE optimization problem as a nonconcave fractional programming problem in cooperative scheme and propose an optimization algorithm with lower complexity to achieve optimal time allocation.
3) Simulation results verify the theoretical analysis of the proposed two computation offloading schemes. Compared with the noncooperative scheme, our user cooperation scheme greatly improves the EE of wireless powered MEC systems and effectively eliminates the doubly near–far effect.

The rest of this paper is organized as follows. In Section II, we present two system models to guarantee the fairness and total energy-efficiency of MEC system, respectively. In Section III, we formulate the EE minimization problem and achieve the optimal time allocation utilizing binary search method. In Section IV, we outline the proposed user cooperation framework and optimize the total EE of system through integrating Dinkelbach's method and Lagrangian dual decomposition method. Then, Section V provides simulation results. Finally, Section VI concludes this paper and provides future directions.

[1] In this paper, we use device and user interchangeably.

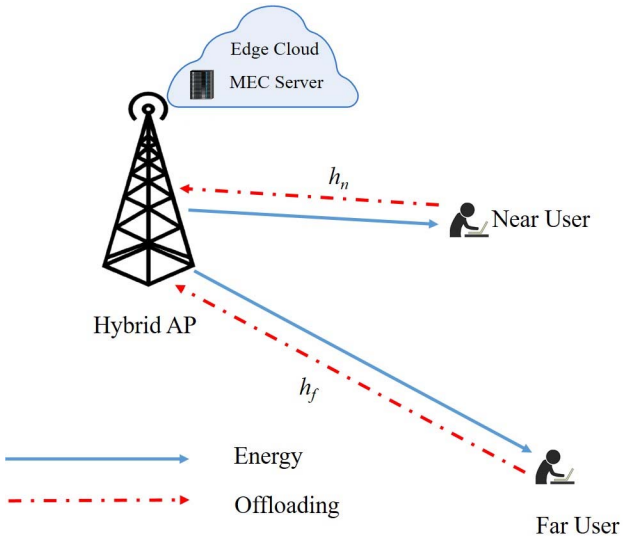

Fig. 1. Two-user WPT-MEC system model in DT mode.

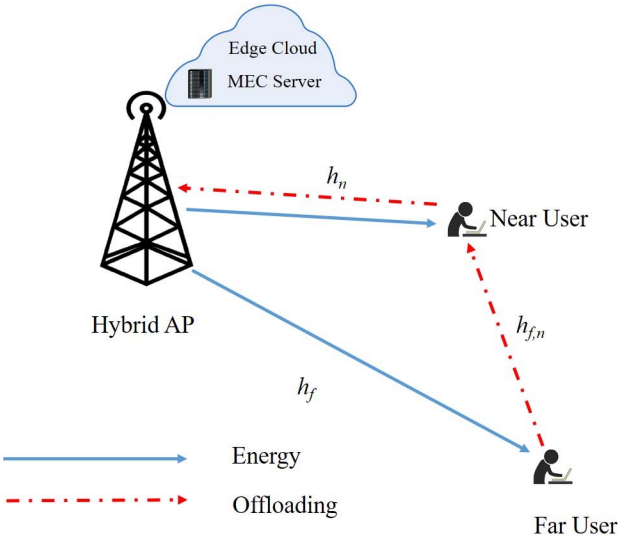

Fig. 2. Two-user WPT-MEC system model in RT mode.

II. System Model

As shown in Figs. 1 and 2, our considered model consists of a dedicated HAP connected with an edge cloud and two typical MDs at different distances in direct transmission (DT) and relay transmission (RT) modes. The MDs can harvest the energy by the WPT from the HAP. Here, HAP has a constant power supply and acts as a power station. The proposed systems has a doubly near–far problem, which is because NU is closer to the HAP than the FU, who has better channel gain, harvests more energy and transmits more information. A block-based TDMA scheme is adopted where each block has a duration of T seconds, which is divided into two phases, i.e., WPT phase and offloading phase. In the first τ_0 time slots, namely charging time, the two users harvest wireless energy from HAP simultaneously. And in the subsequent time slots, i.e., uploading time, which is divided into τ_f and τ_n, NU and FU offload their tasks onto the edge cloud using the harvested energy in WPT phase. Table I summarizes the used notations

TABLE I
List of Notations

Notation	Definition
P_0	Transmission power of the HAP
P_c	Static circuit power
T	Time slots for energy harvesting
W	Channel bandwidth
U_i	The user i
C_i	Battery capacity of U_i
α	Loss exponent
τ_0	Time slots during WET phase
σ_0^2	Noise power at HAP
$d_{f,n}$	The distance of FU and NU
$h_{f,n}$	Channel gain from FU to NU
$\sigma_{f,n}^2$	Noise power at user n
P_i^k	Transmission power of U_i's terminal in k model
E_i	Harvested energy of U_i
d_i	The distance of HAP and U_i
h_i	Channel power gain of U_i
ξ_i	Energy harvesting efficiency of U_i
τ_i	Time slots during offloading phase
θ_i	Portion used to offload of U_i
γ_i^{DT}	Signal to noise ratio of U_i in DT model
R_i^{DT}	Achievable rate of U_i in DT model
$\gamma_{n,HAP,j}^{RT}$	Signal to noise ratio of U_n in jth time slot
$R_{n,HAP,j}^{RT}$	Achievable rate of U_n in jth time slot
η_i^{DT}	Energy efficiency of U_i in DT mode
η^{RT}	Energy efficiency in RT mode

and the corresponding definition in this paper. We introduce the two phases in the next sections.

A. Wireless Power Transfer Phase

In this proposed system, we adopt a simplified channel model that has been widely used in many classical WPCN models [28], [29]. The channel model incorporates small-scale Rayleigh fading with large-scale power attenuation by using the loss exponent $\alpha > 2$, where channel gain remains constant during each block time, but can vary from one block to another. Then, the channel gain h is expressed as

$$h = \begin{cases} \rho\sqrt{G_0\left(\frac{D}{D_0}\right)^{-\alpha}}, & D > D_0 \\ \rho\sqrt{G_0}, & \text{otherwise} \end{cases} \quad (1)$$

where $\rho \sim \mathcal{CN}(0,1)$ is an independent and identically distributed circularly symmetric complex Gaussian (CSCG) random variable with a zero mean and unit variance modeling the small-scale Rayleigh fading, and G_0 is the constant attenuation because of the path loss at a reference distance D_0. Assuming that channel state information (CSI) at users is available, the harvested energy of the user U_i in WPT phase, can be expressed as

$$E_i = \xi_i P_0 h_i^2 \tau_0, \quad i \in \{n, f\} \quad (2)$$

where E_i indicates the harvested energy of U_i, ξ_i denotes EH efficiency of U_i, P_0 is transmit power of the HAP, h_i represents channel power gain from the HAP to U_i.

B. Offloading Phase

As shown in Fig. 1, the MDs offload their computation-intensive tasks to the HAP using the individually harvested energy, which is named DT mode. In order to eliminate the

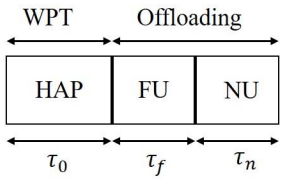

Fig. 3. Frame structure for WPT and offloading phase in a two-user WPT-MEC in DT mode.

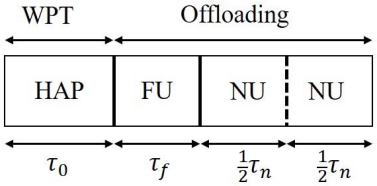

Fig. 4. Frame structure for WPT and offloading phase in a two-user WPT-MEC in RT mode.

doubly near–far effect, as shown in Fig. 2, an RT mode is proposed, in which the NU forwards FU's tasks to HAP for improving the offloading[2] efficiency. To complete users' computation offloading at the rate satisfying QoS requirement, the FU can select a transmission mode from the above two strategies. Next, we will explain two modes in detail.

1) Direct Transmission Mode: Fig. 1 shows offloading policy of DT mode, which pays attention to user fairness. The frame structure for a two-user WPT-MEC in DT mode is illustrated in Fig. 3. For convenience, the total time duration of the frame is assumed to be 1. After harvesting energy, FU and NU offload sequentially their tasks to HAP in next τ_f and τ_n. Therefore, the transmission power of U_i in DT mode can be approximated as

$$P_i^{\mathrm{DT}} = \frac{\theta_i E_i}{\tau_i} = \frac{\theta_i P_0 \xi_i h_i^2 \tau_0}{\tau_i},\ \ i \in \{n, f\} \tag{3}$$

where $0 \le \theta_i \le 1$ denotes the portion of the harvested energy used for computation offloading and τ_i is uploading time of user i. We denote $x_i \sim \mathcal{CN}(0, 1)$ as the signal transmitted by U_i during the offloading time, where $\mathcal{CN}(\mu, \sigma^2)$ stands for a CSCG random variable with mean μ and variance σ^2. The sampled baseband signal can be written as

$$y_{i,\mathrm{HAP}}^{\mathrm{DT}} = h_i \sqrt{P_i^{\mathrm{DT}}} x_i + z_0,\ \ i \in \{n, f\} \tag{4}$$

where $z_0 \sim \mathcal{CN}(0, \sigma_0^2)$ indicates the overall additive Gaussian noise due to the receiving antenna and RF band to baseband signal conversion. Therefore, the signal to noise ratio (SNR) can be obtained as

$$\gamma_{i,\mathrm{HAP}}^{\mathrm{DT}} = \frac{P_i^{\mathrm{DT}} h_i^2}{\sigma_0^2} = \frac{\theta_i P_0 \xi_i h_i^4 \tau_0}{\tau_i \sigma_0^2},\ \ i \in \{n, f\}. \tag{5}$$

Finally, the achievable rate from user i to the HAP is given by

$$R_i^{\mathrm{DT}} = \tau_i \log_2\left(1 + \gamma_{i,\mathrm{HAP}}^{\mathrm{DT}}\right),\ \ i \in \{n, f\}. \tag{6}$$

[2]Due to the relatively high speed of edge clouds, we only consider uploading rather than downloading. It means that the offloading and uploading can be used interchangeably in this paper.

2) Relay Transmission Mode: As we can see in Fig. 2, to eliminate the doubly near–far effect, the NU forwards the FU's information to the HAP, as a relay, using its harvested energy. The frame structure for a two-user WPT-MEC system in RT mode is illustrated in Fig. 4. The FU transmits data to NU during τ_f. In the next time slot $(1/2)\tau_n$, NU is paid[3] to forward FU's tasks to the HAP and offload its own computation tasks to the HAP in the remaining time. Thus, the transmission power of U_i in RT mode can be approximated as

$$P_i^{\mathrm{RT}} = \frac{\theta_i E_i}{\tau_i} = \frac{\theta_i P_0 \xi_i h_i^2 \tau_0}{\tau_i},\ \ i \in \{n, f\}. \tag{7}$$

The channel model is blocking fading and quasistatic. Therefore, NU's received signal in RT mode is

$$y_n^{\mathrm{RT}} = h_{f,n} \sqrt{P_f^{\mathrm{RT}}} x_f + z_{f,n} \tag{8}$$

where $h_{f,n}$ is channel gain from FU to NU, $z_{f,n} \sim \mathcal{CN}(0, \sigma_{f,n}^2)$ indicates the overall additive Gaussian noise due to the receiving antenna and RF band to baseband signal conversion. NF amplifies the received signals and forwards them to the HAP. The signal received at the HAP during slot τ_f is then given by

$$\begin{aligned} y_{n,\mathrm{HAP},1}^{\mathrm{RT}} &= \frac{h_n \sqrt{P_n^{\mathrm{RT}}} y_n^{\mathrm{RT}}}{\sqrt{h_{f,n}^2 P_f^{\mathrm{RT}} + \sigma_{f,n}^2}} + z_0 \\ &= \frac{h_n \sqrt{P_n^{\mathrm{RT}}} \left(h_{f,n} \sqrt{P_f^{\mathrm{RT}}} x_f + z_n\right)}{\sqrt{h_{f,n}^2 P_f^{\mathrm{RT}} + \sigma_{f,n}^2}} + z_0 \\ &= \frac{h_n \sqrt{P_n^{\mathrm{RT}}} h_{f,n} \sqrt{P_f^{\mathrm{RT}}} x_f}{\sqrt{h_{f,n}^2 P_f^{\mathrm{RT}} + \sigma_{f,n}^2}} + \left(\frac{h_n \sqrt{P_n^{\mathrm{RT}}}}{\sqrt{h_{f,n}^2 P_f^{\mathrm{RT}} + \sigma_{f,n}^2}} z_n + z_0\right) \end{aligned} \tag{9}$$

where the expression within the first parentheses indicates the signal part and the second parentheses include the noise part. Therefore, the SNR at HAP from NU in the first half slot $(1/2)\tau_n$ can be obtained as

$$\gamma_{n,\mathrm{HAP},1}^{\mathrm{RT}} = \frac{\frac{P_f^{\mathrm{RT}} P_n^{\mathrm{RT}} h_n^2 h_{f,n}^2}{h_{f,n}^2 P_f^{\mathrm{RT}} + \sigma_{f,n}^2}}{\frac{P_n^{\mathrm{RT}} h_n^2}{h_{f,n}^2 P_f^{\mathrm{RT}} + \sigma_{f,n}^2} + \sigma_0^2} \approx \frac{P_f^{\mathrm{RT}} P_n^{\mathrm{RT}} h_n^2 h_{f,n}^2}{P_n^{\mathrm{RT}} h_n^2 + h_{f,n}^2 P_f^{\mathrm{RT}} \sigma_0^2}. \tag{10}$$

Then, the achievable rate from NU forwarding FU's tasks to the HAP is given by

$$R_{n,\mathrm{HAP},1}^{\mathrm{RT}} = \frac{1}{2} \tau_n \log_2\left(1 + \gamma_{n,\mathrm{HAP},1}^{\mathrm{RT}}\right). \tag{11}$$

Next, NU transfers its own data to HAP and HAP's received signal is

$$y_{n,\mathrm{HAP},2}^{\mathrm{RT}} = h_n \sqrt{P_n^{\mathrm{RT}}} x_n + z_0. \tag{12}$$

Therefore, the SNR at HAP from NU in its next half slot $(1/2)\tau_n$ can be obtained as

$$\gamma_{n,\mathrm{HAP},2}^{\mathrm{RT}} = \frac{P_n^{\mathrm{RT}} h_n^2}{\sigma_0^2}. \tag{13}$$

[3]It is obvious that NU will spend his energy and time on cooperation to attain optimal system EE. Hence, incentive mechanisms should be used in proposed system but it's not the focus of this paper.

Finally, the achievable rate from NU offloading its own tasks to the HAP is given by

$$R_{n,\mathrm{HAP},2}^{\mathrm{RT}} = \frac{1}{2}\tau_n \log_2\left(1+\gamma_{n,\mathrm{HAP},2}^{\mathrm{RT}}\right). \tag{14}$$

C. Energy Efficiency

EE of the user U_i in DT mode is defined as the ratio of the user throughput to its harvested energy and is given by

$$\eta_i^{\mathrm{DT}}(\tau_0,\tau_i) = \frac{R_i^{\mathrm{DT}}(\tau_0,\tau_i)}{E_i^{\mathrm{DT}}(\tau_0,\tau_i)} \tag{15}$$

where E_i^{DT} is total energy consumption of U_i, and can be modeled as

$$E_i^{\mathrm{DT}}(\tau_0,\tau_i) = \left(P_i^{\mathrm{DT}}+Q_i\right)\tau_i = \theta_i P_0 \xi_i h_i^2 \tau_0 + Q_i\tau_i \tag{16}$$

where $0 \le Q_i \le (1-\theta_i)(E_i^{\mathrm{DT}}/\tau_i)$ is the constant energy consumption. In the RT mode, the EE is given by

$$\eta^{\mathrm{RT}} = \frac{R^{\mathrm{RT}}(\tau_0,\tau_i)}{E_{\mathrm{total}}^{\mathrm{RT}}(\tau_0,\tau_i)} \tag{17}$$

where the total throughput and the total energy consumption which are not used to supply for offloading of the system are respectively, formulated as

$$R^{\mathrm{RT}}(\tau_0,\tau_i) = \sum_{j=1}^{2} R_{n,\mathrm{HAP},j}^{\mathrm{RT}}(\tau_0,\tau_i) \tag{18}$$

and

$$E_{\mathrm{total}}^{\mathrm{RT}}(\tau_0,\tau_i) = P_0 - \sum_{i=1}^{2} E_i^{\mathrm{RT}} \tag{19}$$

where the $E_i^{\mathrm{RT}} = \xi_i P_0 h_i^2 \tau_0$. Especially, the energy consumption in HAP during one block time is $E_0 = P_0(\tau_0+\tau_n+\tau_f)$. Due to $\tau_0+\tau_n+\tau_f = 1$, it can be simplified to (19).

III. Max-Min Energy Efficiency Formulation and Optimization in DT Mode

In this section, we consider maximization minimum user's EE (MMUEE) problem. In our system, as we know, MDs first harvest wireless energy in charging time slot and then offload their tasks in offloading time slot. It means that more charging time leads to insufficient time for IT, resulting in lower throughput. It means that excessive time is spent for WPT, which results in low EE at the same transmission power. Otherwise, less charging time will lead to less harvested energy. It means that for the improvement of system EE, it is crucial to allocate time resources rationally. Hence, considering fairness between users, we present the time resource allocation scheme to maximize the individual EE of each user in DT mode, based on the max-min criterion. Our MMUEE problem is formulated as

$$\mathbf{OPT-1}: \max_{\tau_0,\tau_i} \min_{i\in\{f,n\}} \eta_i^{\mathrm{DT}}(\tau_0,\tau_i) \tag{20}$$

subject to

$$C1: \sum_j \tau_j = 1, 0 \le \tau_j \le 1, j \in \{0,f,n\}$$

$$C2: R_i^{\mathrm{DT}} \ge r_i^{\mathrm{DT}}, i \in \{f,n\}$$

$$C3: E_i \le C_i, i \in \{f,n\}$$

where constraint $C1$ denotes the range of time slots τ_0 and τ_i, $C2$ reflects the requirement that the minimum rate satisfies Qos and $C3$ ensures that the maximum harvested energy should is no more than battery capacity. The feasible region for optimization variable τ_0 and τ_i is given by constraints $C1$–$C3$.

Let $\eta^{\mathrm{DT}}(\tau_0,\tau_i) = \min_{i\in\{f,n\}}([R_i^{\mathrm{DT}}(\tau_0,\tau_i)]/[E_i^{\mathrm{DT}}(\tau_0,\tau_i)])$. Then, the $\mathbf{OPT-1}$ is transformed into

$$\overline{\mathbf{OPT-1}}: \max_{\tau_0,\tau_i,\eta^{\mathrm{DT}}} \eta^{\mathrm{DT}} \tag{21}$$

subject to

$$C1 \backsim C3$$

$$C4: \frac{R_i^{\mathrm{DT}}(\tau_0,\tau_i)}{E_i^{\mathrm{DT}}(\tau_0,\tau_i)} \ge \eta^{\mathrm{DT}}.$$

Lemma 1: When the above MMUEE problem achieves optimal solution, the constraint $C4$ should take equality.

Proof: Please refer to Appendix A. ∎

It is not difficult to observe from Lemma 1 that the system achieves optimal EE when both users have equal EE. Intuitively, when we fix the charging time, reducing the uploading time of the user with higher EE will increase the uploading time of other users with lower EE. An effective way we acquire optimal EE of users is that every user attains the same EE. Furthermore, the optimal solution of $\overline{\mathbf{OPT-1}}$ must satisfy the following equation:

$$\eta^{DT*} = \frac{\tau_i^* \log_2\left(1+\frac{\theta_i P_0 \xi_i h_i^4 \tau_0^*}{\tau_i^* \sigma_i^2}\right)}{\theta_i P_0 \xi_i h_i^2 \tau_0^* + Q_i \tau_i^*}. \tag{22}$$

Given η^{DT}, problem $\overline{\mathbf{OPT-1}}$ is feasible if we can find $\boldsymbol{\tau} = (\tau_0,\tau_f,\tau_n)$ such that $\sum_j \tau_j = 1$. Refer to [30], we can obtain τ_0^* using (22) and η^{DT*} by bisection method. Algorithm 1 summarizes the process of finding the optimal value. In particular, we define δ as the maximum tolerance, which is a sufficiently small positive number to hold $\sum_j \tau_j$ closer to 1 as far as possible. Δ is a proper step size to iterate the charging time.

IV. Energy Efficiency Formulation and Optimization in RT Mode

In this section, we consider the system energy-efficiency maximization in RT mode. We first formulate the maximization problem with three constraints. Second, we prove quasi-concavity of objective function (OF). By applying Dinkelbach's method, the original quasi-concavity fractional programming problem is transformed into convex optimization problem in a subtraction form. Finally, by using classical Lagrangian method, Newton iteration method, and subgradient algorithm, we obtain the optimal solution of the transformed problem.

A. Problem Formulation

In RT mode, NU plays the role of a relay, forwarding FU's tasks in half of time slot τ_n. According to the equation $\tau_0+\tau_n+\tau_f = 1$, assuming that τ_0 is fixed, if we reduce

Algorithm 1 Algorithm for the MMUEE Problem in (20)

Set the maximum tolerance δ and the proper step size Δ;
Set η_{min} and η_{max} such that $\hat{\eta}_i^{DT} \in [\eta_{\min}, \eta_{\max}]$.
repeat
  update $\eta = \frac{1}{2}(\eta_{\min} + \eta_{\max})$.
  $\tau_0 = 0$.
  while $\tau_0 \in \{0, 1\}$ **do**
    Compute τ_i and $\sum_j \tau_j$ using (22);
    If $0 \le 1 - \sum_j \tau_j \le \delta$, set $\tau_i^* = \tau_i$ and $\tau_0^* = \tau_0$.
    $\tau_0 \leftarrow \tau_0 + \Delta$.
  end while
  If $\sum_j \tau_j \le 1$, set $\eta_{min} = \eta$. Otherwise, set $\eta_{max} = \eta$.
until $\eta_{\max} - \eta_{\min} \le \epsilon$, where ϵ is the solution accuracy.
return

(or increase) the uploading time of FU excessively, NU will have more (or less) time to forward and upload tasks to the edge cloud. Thus, the total throughput and EE may be smaller due to unconscionable time allocation. Similarly, redundant charging time τ_0 will result in too much harvested energy but cause lower offloading rate. As a result, there are two tradeoffs, i.e., one is the tradeoff between charging and offloading time, and the other is the tradeoff between FU's and NU's uploading time. However, compared to user fairness, it is more meaningful to consider the EE of the entire system in RT mode. This is because that cooperative users aim at eliminating double near–far effect instead of individual EE maximization. Consequently, we present a time resource allocation scheme to maximize the EE of the whole system, which is formulated as

$$\mathbf{OPT-2}: \max_{\boldsymbol{\tau}} \ \eta^{\mathrm{RT}}(\boldsymbol{\tau}). \tag{23}$$

Subject to

$$D1: \sum_j \tau_j = 1, 0 \le \tau_j \le 1, j \in \{0, f, n\}$$
$$D2: R_{n,\mathrm{HAP},l}^{\mathrm{RT}} \ge r_{n,\mathrm{HAP},l}^{\mathrm{RT}}, l = 1, 2$$
$$D3: E_i \le C_i, i \in \{f, n\}$$

where constraint $D1$ is the range condition of time slots τ_0 and τ_i, $D2$ specifies the requirement that the minimum rate should satisfy QoS and $D3$ ensures that the harvested maximum energy should be no more than battery capacity. The feasible region for the optimization variable τ_0, τ_f, and τ_n is given by constraints $D1$–$D3$. Fortunately, we can reduce the number of variables by utilizing the constraint $D1$. In the meantime, the constraint $D3$ can be simplified to a constant constraint independent of variables. Hence, the origin problem $\mathbf{OPT-2}$ is converted into $\overline{\mathbf{OPT-2}}$ as follows:

$$\overline{\mathbf{OPT-2}}: \max_{\tau_0, \tau_n} \ \eta^{\mathrm{RT}}(\tau_0, \tau_n). \tag{24}$$

Subject to

$$\overline{D}1: 0 \le \tau_0, \tau_n \le 1$$
$$\overline{D}2: R_{n,\mathrm{HAP},l}^{\mathrm{RT}} \ge r_{n,\mathrm{HAP},l}^{\mathrm{RT}}, l = 1, 2$$
$$\overline{D}3: E_i \le C_i, i \in \{f, n\}.$$

B. Quasi-Concavity of Objective Function in RT Mode

In the section, the quasi-concavity of the OF in $\overline{\mathbf{OPT-2}}$ will be discussed in Lemmas 2 and 3.

Lemma 2: When $(\sigma_0^2/[\theta_n P_0 \xi_n h_n^4]) \ge (1/[\theta_f P_0 \xi_f h_f^2 h_{f,n}^2])$, the $R_{n,\mathrm{HAP},1}^{\mathrm{RT}}$ is a jointly concave function with respect to time slots τ_0 and τ_n.

Proof: Please refer to Appendix B. ∎

Observing Lemma 2, we can see that the channel condition between FU and NU must be good enough to make RT practical. This is due to the fact that the RT leads to squander energy and transmit less data in poor channel condition.

Lemma 3: The OF in $\overline{\mathbf{OPT-2}}$ is jointly quasi-concavity with respect to time slots τ_0 and τ_n.

Proof: With reference to Lemma 2, it's obvious that $R_{n,\mathrm{HAP},2}^{\mathrm{RT}}$ is a concave function with respect to time slots τ. $R_{n,\mathrm{HAP},1}^{\mathrm{RT}} + R_{n,\mathrm{HAP},2}^{\mathrm{RT}}$ is also a concave function since it is the summation of $R_{n,\mathrm{HAP},i}^{\mathrm{RT}}$s. In addition, the denominator $E_{\mathrm{HAP}}^{\mathrm{RT}}$ is both affine and positive with respect to charging time τ_0, since it is the linear combination of multiple non-negative variables and a positive constant. Hence, the OF in $\overline{\mathbf{OPT-2}}$ is a quasi-concavity with respect to time slots τ_0 and τ_n. ∎

Quasi-concavity [31] can be considered as a generalized concavity, since it can describe discontinuous functions as well as functions with multiple stationary points. It means that a local maximum is not ensured to be a global maximum and thus standard convex optimization techniques (e.g., interior-point and ellipsoid methods), cannot be directly used for obtaining the optimal solution. From the above discussion, we can know that our proposed EE maximization problem $\overline{\mathbf{OPT-2}}$ is concave-convex fractional optimization problem, which belongs to a special nonlinear fractional programming and can share important properties with convex optimization theory. By using Dinklebach's method, a concave-convex fractional programming can be transformed into a convex optimization problem and be solved with the aid of classical methods in convex optimization theory. In the next section, we will introduce Dinklebach's method.

C. Dinkelbach's Method

Dinkelbach's method is an iterative algorithm that can be applied for solving a quasi-concave problem in a parameterized concave form. In order to solve the $\overline{\mathbf{OPT-2}}$, we adopt the following main theorem from the nonlinear fractional programming theory [32]. Similar to Theorem 1, the OF in $\overline{\mathbf{OPT-2}}$ can be written as $F(\eta^{\mathrm{RT}}) = R^{\mathrm{RT}} - \eta^{\mathrm{RT}} E_{\mathrm{total}}^{\mathrm{RT}}$, which is concave. In order to intuitively understand η^{RT}, it can be viewed as the "price" of energy, which is a negative weight on the total power consumption of system. At the optimal OF value of $\eta^{\mathrm{RT}*}$, the following holds true: $\max\{F(\eta^{\mathrm{RT}*})\} = \max\{R^{\mathrm{RT}} - \eta^{\mathrm{RT}*} E_{\mathrm{total}}^{\mathrm{RT}}\} = 0$. Definitely, the solution of $\max\{F(\eta^{\mathrm{RT}*})\}$ is equivalent to the solution of the fractional $\overline{\mathbf{OPT-2}}$. Dinkelbach's method is summarized in Algorithm 2. It is not difficult to obtain that the time complexity of Algorithm 2 is $O(L_{\max}^{\mathrm{outer}} * L_{\max}^{\mathrm{inner}})$, where $L_{\max}^{\mathrm{outer}}$ denotes the maximum number of iterations for Dinkelbach's method and $L_{\max}^{\mathrm{inner}}$ indicates the number of iterations for subgradient method. For further details and a proof of convergence, please refer to [33].

Algorithm 2 Dinkelbach's Method for EE Maximization

1: Input: $L_{\max}^{outer}$: the maximum number of iterations and ϵ^{outer} : the maximum tolerance;
2: $\eta_0^{RT} \leftarrow 0$;
3: $i \leftarrow 0$;
4: **while** $i \le L_{\max}^{outer}$ or $|\eta_i^{RT} - \eta_{i-1}^{RT}| > \varepsilon^{outer}$ **do**
5: $i \leftarrow i + 1$;
6: Obtain the optimal charging time τ_0^* and offloading time τ_n^* (inner loop) by solving $\mathbf{OPT-3}$.
7: $\eta_i^{RT*} \leftarrow \frac{R^{RT}(\tau_0^*, \tau_n^*)}{E_{total}^{RT}(\tau_0^*, \tau_n^*)}$;
8: **end while**
9: **return**

D. Proposed Algorithm for Solving the OP in RT Mode

In this section, we mainly focus on solving the proposed optimization problem by applying Dinkelbach's method and Lagrangian dual decomposition method.

According to the formulated fractional $\overline{\mathbf{OPT-2}}$ and applying Dinkelbach's method discussed in above section, the parametric version of the EE-maximization $\overline{\mathbf{OPT-2}}$ is reformulated as

$$\mathbf{OPT-3}: \max_{\tau_0, \tau_n} \left\{R^{\mathrm{RT}} - \eta^{\mathrm{RT}} E_{\mathrm{total}}^{\mathrm{RT}}\right\}. \tag{25}$$

Subject to

$$\overline{D}1 \sim \overline{D}3$$

where $R^{\mathrm{RT}}(\tau_0, \tau_n)$ with respect to optimization variable τ_0 and τ_n, is concave, respectively. $E_{\mathrm{total}}^{\mathrm{RT}}(\tau_0, \tau_n)$ is positive and affine. Then, the OF is concave and the feasible region generated by constraints $\overline{D}1 \sim \overline{D}3$ is a convex set. Thus, $\mathbf{OPT-3}$ is a convex optimization problem. Furthermore, we can obtain the primal solution with a zero duality gap by solving a dual problem. In the following, the Lagrangian function over variable τ_0 and τ_n for optimization $\mathbf{OPT-3}$ is presented by

$$\begin{aligned} L\{\tau_0, \tau_n, \boldsymbol{\lambda}, \boldsymbol{\mu}\} = {} & R^{\mathrm{RT}} - \eta E_{\mathrm{total}}^{\mathrm{RT}} + \mu_1\big(C_f - E_f\big) + \mu_2(C_n - E_n) \\ & + \lambda_1\big(R_{n,\mathrm{HAP},1}^{\mathrm{RT}} - r_{n,\mathrm{HAP},1}^{\mathrm{RT}}\big) \\ & + \lambda_2\big(R_{n,\mathrm{HAP},2}^{\mathrm{RT}} - r_{n,\mathrm{HAP},2}^{\mathrm{RT}}\big). \end{aligned} \tag{26}$$

Since $\mathbf{OPT-3}$ is a standard form of the convex optimization problem, we can deal with the updating process of the primal and dual variables in terms of the Karush–Kuhn–Tucker first order optimality conditions, in order to find the optimal solution. In the following, we mainly focus on updating optimization variables and Lagrangian multiplier to obtain the solution.

1) Optimal Time Slots for RT Mode: According to the above discussion, we can calculate the first order partial derivation equals zero with respect to τ_0 and τ_n, respectively as follows, which is given by:

$$\begin{aligned} \frac{\partial L}{\partial \tau_0} = {} & \frac{1}{2\ln 2}\frac{(\lambda_2+1)\tau_n}{\tau_0 + \big(M + B^{-1}\big)\tau_n} \\ & + \frac{1}{2\ln 2}\frac{(\lambda_1+1)\big[B^{-1} + M\tau_n\big]\tau_n}{\big[B^{-1} + \big(1 - B^{-1}\big)\tau_0 + M\tau_n\big]\big[B^{-1} - B^{-1}\tau_0 + M\tau_n\big]} \\ & + (\eta - \mu_1)P_0\xi_f h_f^2 + (\eta - \mu_2)P_0\xi_n h_n^2 = 0 \end{aligned} \tag{27}$$

and

$$\begin{aligned} \frac{\partial L}{\partial \tau_n} = {} & \frac{(\lambda_1+1)}{2}\log_2\left(1 + \frac{\tau_0}{B^{-1} - B^{-1}\tau_0 + M\tau_n}\right) \\ & - \frac{(\lambda_1+1)M\tau_0\tau_n}{2\ln 2\big[B^{-1} + \big(1 - B^{-1}\big)\tau_0 + M\tau_n\big]\big[B^{-1} - B^{-1}\tau_0 + M\tau_n\big]} \\ & + \frac{(\lambda_2+1)}{2}\log_2\left(1 + \frac{\tau_0}{\big(M + B^{-1}\big)\tau_n}\right) - \frac{(\lambda_2+1)\tau_0}{2\big[\tau_0 + \big(M + B^{-1}\big)\tau_n\big]} \\ = {} & 0 \end{aligned} \tag{28}$$

where $M = (\sigma_0^2/A) - (1/B)$ and $B^{-1} = (1/B)$. Particularly, M is a priority indicator including channel gains in three different links (i.e., h_f, h_f, and $h_{f,n}$), to some extent, which represents users' willingness to cooperate. Poor channel condition between FU and NU causes collaboration failure. However, it is not practical to calculate the optimal τ_0^* and τ_n^* directly. Especially, (27) and (28) are transcendental equations, and in general they do not have closed-form solution. Hence, we can only get their approximate solution by Newton iteration method [34]. For example, we can observe that the optimal time slot τ_n^* is the solution of (27), i.e., the intersection point between two equations, $\varphi(\tau_n)$ and $\psi(\tau_n)$, which can be given by

$$\varphi(\tau_n) = \frac{(\lambda_1+1)\big[B^{-1} + M\tau_n\big]\tau_n}{\big[B^{-1} + \big(1 - B^{-1}\big)\tau_0 + M\tau_n\big]\big[B^{-1} - B^{-1}\tau_0 + M\tau_n\big]} \tag{29}$$

and

$$\psi(\tau_n) = 2\ln 2(\upsilon - \eta)P_0\Big(\xi_n h_n^2 + \xi_f h_f^2\Big) - \frac{(\lambda_2+1)\tau_n}{\tau_0 + \big(M + B^{-1}\big)\tau_n}. \tag{30}$$

Then, the time slot τ_n is updated iteratively by

$$\tau_n(t+1) = \tau_n(t) - \frac{\varphi(\tau_n(t)) - \psi(\tau_n(t))}{\varphi'(\tau_n(t)) - \psi'(\tau_n(t))} \tag{31}$$

where $\varphi'(\cdot)$ and $\psi'(\cdot)$ denote the first-order derivative with respect to $\tau_n(t)$. Refer to [35], Newton iteration method usually converges, if this initial value $\tau_n(0)$ is close enough to the zero τ_n^*, and if $\varphi'(\tau_n(t)) \neq \psi'(\tau_n(t))$. Furthermore, for the equation with a simple root, the convergence is at least quadratic in a neighbourhood of the zero.

Analyzing (27) and (28), we find that the larger M, which means the favorable channel between two users, leads to less charging time and more uploading time used for cooperation.

2) Lagrange Multiplier Update for RT Mode: In this section, we apply the subgradient algorithm to update the dual variables λ, μ, ν, whose equations are presented

$$\begin{aligned} \lambda_1(k+1) &= \big[\lambda_1(k) + \beta_1\big(R_{n,\mathrm{HAP},1}^{\mathrm{RT}} - r_{n,\mathrm{HAP},1}^{\mathrm{RT}}\big)\big]^+ \\ \lambda_2(k+1) &= \big[\lambda_2(k) + \beta_2\big(R_{n,\mathrm{HAP},2}^{\mathrm{RT}} - r_{n,\mathrm{HAP},2}^{\mathrm{RT}}\big)\big]^+ \\ \mu_1(k+1) &= \big[\mu_1(k) + \beta_3\big(C_f - E_f\big)\big]^+ \\ \mu_2(k+1) &= [\mu_2(k) + \beta_4(C_n - E_n)]^+ \end{aligned} \tag{32}$$

where β_1, β_2, β_3, and β_4 denote the proper step size of subgradient iteration, respectively, and $[z]^+$ denotes $\max\{0, z\}$. Our Time allocation Algorithm (inner loop) is summarized in Algorithm 3. It is not difficult to obtain that the time complexity of Algorithm 2 is $O(L_{\max}^{\mathrm{inner}} * L_{\max}^{\mathrm{outer}} * L_{\max}^{\mathrm{Newton}})$, where

Algorithm 3 Time Allocation Algorithm (Inner Loop) for Obtaining τ_0^* and τ_n^*

1: Input: $L_{\max}^{inner}$: the maximum number of iterations and ϵ^{inner} : the maximum tolerance;
2: $k \leftarrow 0$;
3: **while** $k \leq L_{\max}^{inner}$ or $|\lambda_1(k)-\lambda_1(k-1)| > \varepsilon^{inner}$ and $|\lambda_2(k)-\lambda_2(k-1)| > \varepsilon^{inner}$ and $|\mu_1(k)-\mu_1(k-1)| > \varepsilon^{inner}$ and $|\mu_2(k)-\mu_2(k-1)| > \varepsilon^{inner}$ **do**
4: $k \leftarrow k+1$;
5: Obtain the optimal charging time τ_0^* and offloading time τ_n^* by (27) and (28) using Newton iteration method.
6: Update lagrange multiplier $\boldsymbol{\lambda}$ and $\boldsymbol{\mu}$ by (32)
7: **end while**
8: **return**

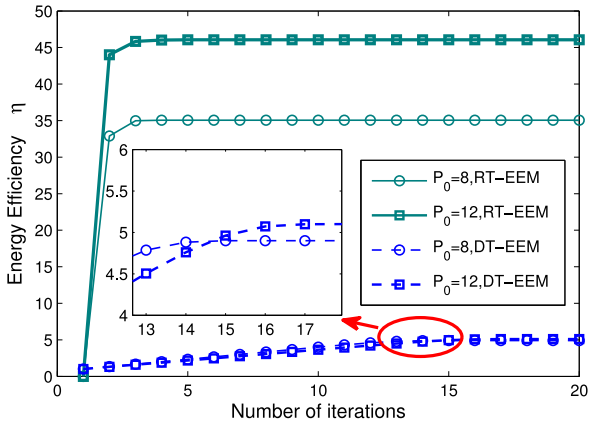

Fig. 5. EE versus number of iterations for different transmission powers.

$L_{\max}^{\text{inner}}$ denotes the maximum number of iterations of updating Lagrangian multipliers, $L_{\max}^{\text{outer}}$ indicate the maximum number of iterations for EE convergence by Dinkelbachs method and $L_{\max}^{\text{Newton}}$ is the maximum number of iterations for obtaining optimal time value by Newton iteration method.

V. Numerical Results and Discussion

In this section, we verify the performance of our algorithm in two different transmission modes (i.e., DT and RT modes) in wireless powered MEC systems according to the practical parameter settings referred in [17], [36], and [37]. To ensure the reliability of the results, several influencing factors are considered in the experimental process, including the noise power and the path loss of transmission links. We will refer to our algorithms in DT and RT modes as "DT-EEM" and "RT-EEM" for short. In addition, we will compare our algorithms with the following three baselines.

1) *UC-JOPT:* The wireless powered computation offloading scheme with user cooperation by jointly optimizing power and time allocation in [17].
2) *UC-SOT:* A simplified wireless powered computation offloading scheme with user cooperation where the entire time is averaged for WPT and offloading phase (i.e., $\tau_0 = \tau_f + \tau_n = 1/2T$). In the experiments, τ_f and τ_n are the optimal solutions obtained from Algorithm 2, but they are suboptimal compared with the solutions by the proposed RT-EEM scheme.
3) *NC-SOT:* A simplified wireless powered computation offloading scheme without user cooperation, which is similar to UC-SOT letting $\tau_0 = \tau_f + \tau_n = 1/2T$. Compared with our DT-EEM, it is a suboptimal non-cooperative time allocation scheme.

Unless otherwise stated, the practical parameter settings are as follows. We consider two Huawei Mate 10 devices with the CPU frequency 2.36 GHz, RAM 4 GB, and ROM 64 GB. The MEC server is DELL OptiPlex 3010 with Quad-core CPU 3.3 GHz and RAM 8 GB. The HAP's transmission power range is from 8 W to 12 W. In our experiments, the channel model incorporates small-scale Rayleigh fading and large-scale power attenuation, where path-loss exponent α is from 3.5 to 4 and noise power is $\sigma_0^2 = -70$ dBm as well as $\sigma_i^2 = -70$ dBm. The normalized duration of each block is $T = 1$ and the reference distance D_0 is 1 m. The distance between HAP and NU, HAP and FU, NU and FU are $d_n = 6$ m, $d_f = 10$ m, and $d_{f,n} = 5$ m, respectively. The EH efficiency $\xi_i = 0.2$ and the portion of the harvested energy used for computation offloading $\theta_i = 0.8$. The harvested energy requirement takes two values as $C_i = 1$ J or 2 J, and the rate requirements are set as $r_i^{\text{DT}} = 200$ kb/s, $r_{n,\text{HAP},1}^{\text{RT}} = 200$ kb/s, and $r_{n,\text{HAP},2}^{\text{RT}} = 200$ kb/s. In fact, those two requirements are set by FU to decide whether to cooperate with NU or not and they are the minimum harvested energy required at FU.

For the sake of fast convergence, we assume that the step size of Lagrangian multiplier update $\beta_1 = \beta_2 = \beta_3 = \beta_4 = 0.05$, the convergence tolerance of iterative algorithms $\varepsilon_{\text{outer}} = \varepsilon_{\text{inner}} = 10^{-5}$, the maximum number of inner loop iterations $L_{\text{outer}} = 110$ and the maximum number of outer loop iterations $L_{\text{inner}} = 30$.

A. Convergence of Iterative Algorithms

In this section, we focus on the EE versus the number of iterations and the convergence speed of our proposed iterative algorithms for two modes, i.e., DT-EEM and RT-EEM, which are depicted in Fig. 5. Specifically, Fig. 5 depicts the EE of the proposed iterative algorithms for different levels of transmission power. We can observe that the larger the transmit power is, the higher the system EE is, in both DT and RT mode, when $P_0 = 8, 12$ W. This is because that higher power results in less energy used for WPT, more offloading time as well as higher throughput.

In addition, our proposed two algorithms can converge within 20 iterations and then the convergence speed is almost unchanged for different transmit powers in DT, RT modes, which is expected for the practical WPT-MEC system. Compared with the DT mode, our algorithm in RT mode has higher EE at the same transmission power. The reason behind the observation is that RT-EEM eliminates the double-near–far effect through user cooperation, and the user with more energy can forward the tasks of the user with less energy to HAP. It means that utilizing cooperation has significant performance improvement over the system without cooperation.

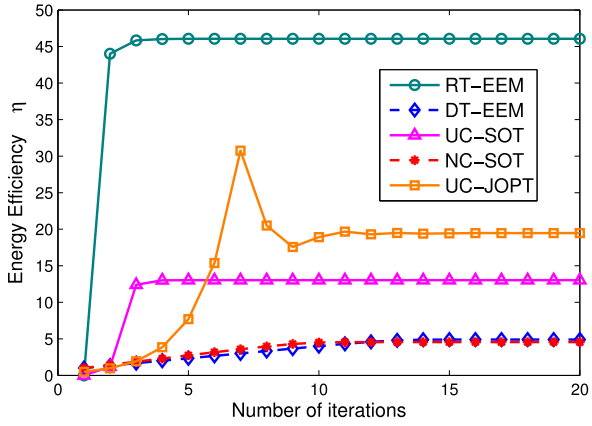

Fig. 6. EE versus number of iterations.

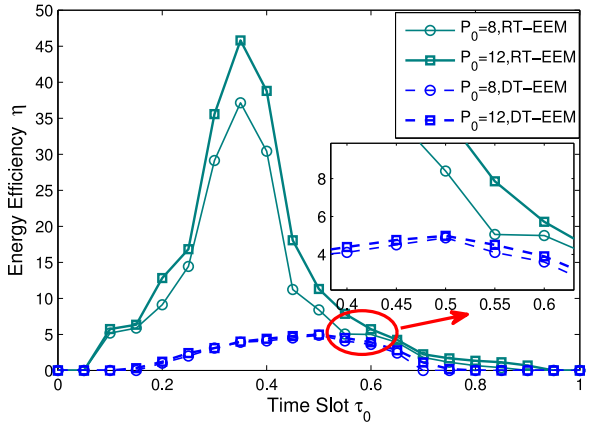

Fig. 7. EE versus charging time for different transmit powers.

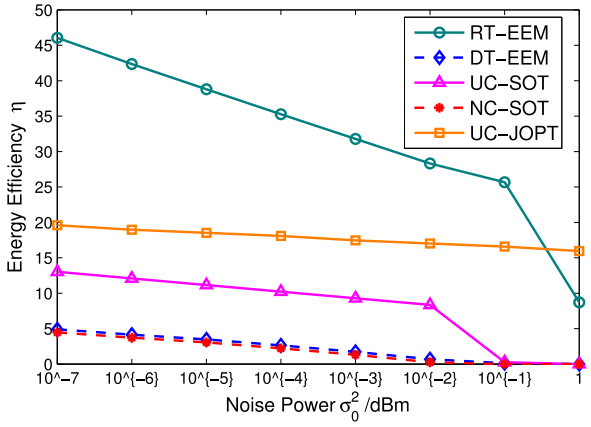

Fig. 8. EE versus noise power.

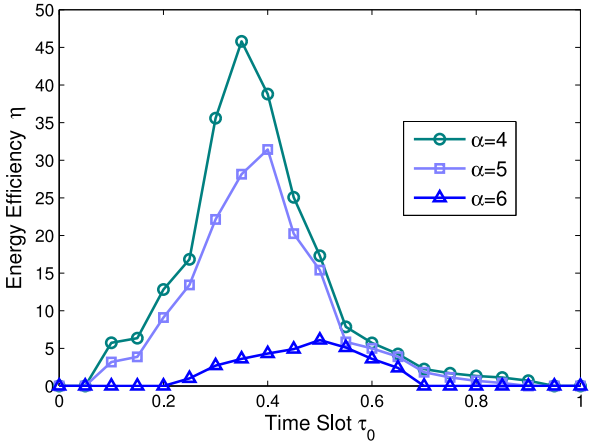

Fig. 9. EE versus charging time with different loss exponent in RT mode.

Fig. 6 depicts the EE comparison of the proposed RT-EEM scheme and three baselines, i.e., UC-JOPT, UC-SOT, and NC-SOT. We can observe that RT-EEM has much higher EE than RT-SOT and DT-EEM outperforms NC-SOT in terms of EE, which means that the optimization for time allocation is effective. In addition, we also find that user cooperation scheme, RT-EEM, is obviously superior to noncooperative one, UC-JOPT. Compared with UC-JOPT, which is composed of two low-complexity bisection search methods, RT-EEM contains three iterative algorithms. However, RT-EEM sacrifices time resource to get higher EE than UC-JOPT. Thus, the proposed RT-EEM scheme can effectively handle the computation-intensive tasks and is suitable for the devices with low battery capacity.

B. Effects of Charging Time on Energy Efficiency

In this section, we explore the effects of charging time on EE in those five algorithms and verify the tradeoff between charging and offloading time, with different transmission powers. Fig. 7 shows the effects of transmit power on EE in five different schemes. Two blue lines show that EE in DT mode increases as the charging time τ_0 increases when τ_0 is small. After EE reaches the peak value ($\tau_0 = 0.48$), it decreases as the time slots increase.

The green lines show that the EE of RT mode increases as the charging time τ_0 increases when τ_0 is small. After EE achieves the peak value ($\tau_0 = 0.35$), it decreases as the time slots increases. This is due to the fact that more time is allocated to guarantee the harvested energy requirement rather than offloading. That variation exactly represents the tradeoff between charging time and offloading time. Within a certain range, the larger transmit power is, the higher EE is.

By comparing that four curves, we can easily find that the EE of the cooperative scheme (i.e., RT mode) is higher and more stable than noncooperative scheme (i.e., DT mode). Consequently, the optimized WPT-MEC system with cooperation has remarkable performance improvement compared with the systems without cooperation.

C. Effects of Channel State Information on Energy Efficiency

In this section, we explore the effects of CSI on EE. Fig. 8 plots the EE curves of five schemes, versus noise powers. Apparently, performance in RT-EEM scheme is preeminent comparing with several other methods in the case of low or high noise. By the comparisons, the DT-EEM and NC-SOT are suitable for channels with high SNR. Compared with noncollaborative schemes, user cooperation schemes are more robust and insensitive to the channel state.

As shown in Fig. 9, we plot the EE curves for different channel gains of our algorithm in RT mode. We can observe that for $\alpha = 4$ the EE increases as the charging time τ_0 increases when

τ_0 is small. After EE achieves the peak value ($\tau_0 = 0.35$), it decreases as the time slots increases.

Another observation is that the larger path loss is, the lower EE of system is. Moreover, due to the effect of channel gain, when loss exponent becomes larger, it requires more charging time τ_0 to get the optimal EE. It is because lower channel gain means less EH during each block time, which requires more charging time in WPT phase in order to achieve optimal EE. On the contrary, excessive charging time will result in lower throughput and EE because of insufficient offloading time. Therefore, the result confirms that the low path loss is beneficial for harvesting energy as well as improving EE.

VI. Conclusion

In this paper, we study the problem of energy-efficient offloading and resource allocation in multiuser wireless powered MEC. To the best of our knowledge, this paper is the first work of integrating offloading with wireless power and resource allocation so as to achieve the maximization of EE under minimum QoS constraint and harvesting energy requirement. We propose two low-complexity time allocation algorithms to achieve the fairness of users in WPT-MEC system and total EE maximization in DT and RT modes, respectively. The simulation results demonstrate that in the WPT-MEC system, user cooperation can significantly improve EE than the systems without cooperation.

For the future work, we will promote our two-user model to multiuser one. Moreover, considering finite storage capacity of MDs, we are going to study the issue of MEC caching (i.e., caching models, caching content regeneration and caching channels). In addition, we will study how to integrate SWIPT with the proposed charging policy so as to achieve the data receiving and wireless charging simultaneously.

Appendix A
Proof of Lemma 1

Before proofing the Lemma 1, we first verify that $G(\tau_i)$ is a monotonically increasing function with $\tau_i (0 \le \tau_i \le 1)$, where $G(\tau_i)$ is expressed as

$$G(\tau_i) = \frac{R_i^{\mathrm{DT}}(\tau_i)}{E_i^{\mathrm{DT}}(\tau_i)} = \frac{\tau_i \log_2\left(1 + \frac{\theta_i P_0 \xi_i h_i^4 \tau_0}{\tau_i \sigma_i^2}\right)}{\theta_i P_0 \xi_i h_i^2 \tau_0 + Q_i \tau_i}. \tag{33}$$

The first-order derivation of $G(\tau_i)$ with respect to τ_i can be given by

$$\frac{\partial G}{\partial \tau_i} = \frac{A_i \log_2\left(1 + \frac{A_i B_i}{\tau_i}\right) - \frac{A_i B_i (A_i + Q_i \tau_i)}{\ln 2 (A_i B_i + \tau_i)}}{(A_i + Q_i \tau_i)^2} \tag{34}$$

where $A_i = \theta_i P_0 \xi_i h_i^2 \tau_0$ and $B_i = (h_i^2/\tau_0)$. Then, we denote $H(\tau_i) = A_i \log_2(1+(A_i B_i/\tau_i)) - ([A_i B_i (A_i + Q_i \tau_i)]/[\ln 2 (A_i B_i + \tau_i)])$. It is obvious that $H(\tau_i)$ is a monotonically decreasing function. When $H(1) \ge 0$, (34) is always greater than zero. Thus, $G(\tau_i)$ is an increasing function of τ_i and the maximum value of η is achieved when two users achieve equal EE. Suppose that U_i has the minimum EE between two users, i.e., $G(\tau_i) > G(\tau_{-i})$.[4] Now we can decrease τ_i and increase τ_{-i} to have a higher minimum EE. This means that the optimal solution is obtained when the equality holds for constraint $C4$.

[4]If $\mathcal{T} = \{\tau_1, \tau_2, \ldots, \tau_i, \ldots, \tau_n\}$, we let $\mathcal{T}_{-i} = \{\tau_1, \ldots, \tau_{i-1}, \tau_{i+1}, \ldots, \tau_n\}$ and $\tau_{-i} \in \mathcal{T}_{-i}$.

Appendix B
Proof of Lemma 2

On the basis of (11), we can obtain

$$R_{n,\mathrm{HAP},1}^{\mathrm{RT}} = \frac{1}{2}\tau_n \log_2\left(1 + \frac{\tau_0}{\frac{1}{B} - \frac{1}{B}\tau_0 + \left(\frac{\sigma_0^2}{A} - \frac{1}{B}\right)\tau_n}\right) \tag{35}$$

where $A = \theta_n P_0 \xi_n h_n^4$ and $B = \theta_f P_0 \xi_f h_f^2 h_{f,n}^2$. In order to show the concavity of $R_{n,\mathrm{HAP},1}^{\mathrm{RT}}$, we first prove the monotonousness of (36) which is expressed as

$$y(x) = 1 + \frac{x}{-\frac{1}{B}x + \left(\frac{\sigma_0^2}{A} - \frac{1}{B}\right)}. \tag{36}$$

The first-order derivation of (36) with respect to x can be calculated as

$$\frac{\partial y}{\partial x} = \frac{\frac{\sigma_0^2}{A} - \frac{1}{B}}{\left[-\frac{1}{B}x + \left(\frac{\sigma_0^2}{A} - \frac{1}{B}\right)\right]^2}. \tag{37}$$

If $([\sigma_0^2/A] - [1/B]) \ge 0$ holds, (37) will be more than zero. Furthermore, the logarithmic function is concave. The scalar composition of convex function ensures the concavity of (38), which is given by

$$f(x) = \log_2\left(1 + \frac{x}{-\frac{1}{B}x + \left(\frac{\sigma_0^2}{A} - \frac{1}{B}\right)}\right). \tag{38}$$

Then, we can obtain that the perspective function [38] of (38) is

$$g(x,t) = t \log_2\left(1 + \frac{\frac{x}{t}}{-\frac{1}{B}\frac{x}{t} + \left(\frac{\sigma_0^2}{A} - \frac{1}{B}\right)}\right). \tag{39}$$

According to the property of perspective function, if the primitive function is convex (or concave) with respect to variable x, the perspective function preserves convexity (or concavity) with respect to joint variables x and t. Hence, the intermediate form is rewritten as

$$F(\tau_0, \tau_n) = \frac{1}{2}\tau_n \log_2\left(1 + \frac{\tau_0}{-\frac{1}{B}\tau_0 + \left(\frac{\sigma_0^2}{A} - \frac{1}{B}\right)\tau_n}\right) \tag{40}$$

which is also a concave function. Denoting $M = (1/B)$ and $N = (\sigma_0^2/A) - (1/B)$, (40) can be converted into

$$F(\tau_0, \tau_n) = \frac{1}{2}\tau_n \log_2\left(1 + \frac{\tau_0}{-M\tau_0 + N\tau_n}\right). \tag{41}$$

Using the operation that preserve concavity of functions, we can construct a concave function which is given by

$$F(\tau_0, \tau_n + K) = \left(1 + K\frac{1}{\tau_n}\right) R^{\mathrm{RT}}_{n,\mathrm{HAP},1}(\tau_0, \tau_n) \tag{42}$$

where $K = (M/N)$. Then, we get

$$R^{\mathrm{RT}}_{n,\mathrm{HAP},1}(\tau_0, \tau_n) = \frac{\tau_n}{\tau_n + K} F(\tau_0, \tau_n + K). \tag{43}$$

Calculating the second-order derivative of $R^{\mathrm{RT}}_{n,\mathrm{HAP},1}(\tau_0, \tau_n)$, Hessian matrix is given by

$$H_{R^{\mathrm{RT}}_{n,\mathrm{HAP},1}} = \frac{\tau_n}{\tau_n + K} H_F + \begin{bmatrix} 0 & \frac{\partial F}{\partial \tau_0} \\ \frac{\partial F}{\partial \tau_0} & 2\frac{\partial F}{\partial \tau_n} - \frac{2F}{\tau_n + K} \end{bmatrix} \frac{K}{(\tau_n + K)^2} \tag{44}$$

which is negative-semidefinite. Thus, $R^{\mathrm{RT}}_{n,\mathrm{HAP},1}(\tau_0, \tau_n)$ is jointly concave with respect to τ_0 and τ_n.

REFERENCES

[1] K. Wang, K. Yang, H.-H. Chen, and L. Zhang, "Computation diversity in emerging networking paradigms," *IEEE Wireless Commun.*, vol. 24, no. 1, pp. 88–94, Feb. 2017.

[2] Mobile Communication Forum. (2018). *5G White Paper 5G Mobile/Multi-Access Edge Computing*. [Online]. Available: http://www.future-forum.org/2009cn/

[3] A. Al-Shuwaili and O. Simeone, "Energy-efficient resource allocation for mobile edge computing-based augmented reality applications," *IEEE Wireless Commun. Lett.*, vol. 6, no. 3, pp. 398–401, Jun. 2017.

[4] C. You, K. Huang, H. Chae, and B.-H. Kim, "Energy-efficient resource allocation for mobile-edge computation offloading," *IEEE Trans. Wireless Commun.*, vol. 16, no. 3, pp. 1397–1411, Mar. 2017.

[5] Z. Kuang, S. Guo, J. Liu, and Y. Yang, "A quick-response framework for multi-user computation offloading in mobile cloud computing," *Future Gener. Comput. Syst.*, vol. 81, pp. 166–176, Apr. 2018.

[6] Y. Mao, J. Zhang, and K. B. Letaief, "Dynamic computation offloading for mobile-edge computing with energy harvesting devices," *IEEE J. Sel. Areas Commun.*, vol. 34, no. 12, pp. 3590–3605, Dec. 2016.

[7] Y. Wu *et al.*, "Dual-connectivity enabled traffic offloading via small cells powered by energy-harvesting," in *Proc. IEEE Glob. Commun. Conf. (GLOBECOM)*, 2018, pp. 1–6.

[8] S. Sudevalayam and P. Kulkarni, "Energy harvesting sensor nodes: Survey and implications," *IEEE Commun. Surveys Tuts.*, vol. 13, no. 3, pp. 443–461, 3rd Quart., 2011.

[9] H. Yu, Y. Zhang, S. Guo, Y. Yang, and L. Ji, "Energy efficiency maximization for WSNs with simultaneous wireless information and power transfer," *Sensors*, vol. 17, no. 8, p. 1906, 2017.

[10] S. Ulukus *et al.*, "Energy harvesting wireless communications: A review of recent advances," *IEEE J. Sel. Areas Commun.*, vol. 33, no. 3, pp. 360–381, Mar. 2015.

[11] D. Zhang *et al.*, "Resource allocation for green cloud radio access networks powered by renewable energy," in *Proc. Glob. Commun. Conf.*, 2017, pp. 1–6.

[12] N. Zhao, F. R. Yu, and V. C. M. Leung, "Wireless energy harvesting in interference alignment networks," *IEEE Commun. Mag.*, vol. 53, no. 6, pp. 72–78, Jun. 2015.

[13] Y. Chen, N. Zhao, and M.-S. Alouini, "Wireless energy harvesting using signals from multiple fading channels," *IEEE Trans. Commun.*, vol. 65, no. 11, pp. 5027–5039, Nov. 2017.

[14] N. Zhao *et al.*, "Artificial noise assisted secure interference networks with wireless power transfer," *IEEE Trans. Veh. Technol.*, vol. 67, no. 2, pp. 1087–1098, Feb. 2018.

[15] S. Bi and Y.-J. A. Zhang, "An ADMM based method for computation rate maximization in wireless powered mobile-edge computing networks," in *Proc. IEEE Int. Conf. Commun. (ICC)*, 2018, pp. 1–7.

[16] F. Zhou, Y. Wu, R. Q. Hu, and Y. Qian, "Computation rate maximization in UAV-enabled wireless powered mobile-edge computing systems," *IEEE J. Sel. Areas Commun.*, vol. 36, no. 9, pp. 1927–1941, 2018.

[17] X. Hu, K. K. Wong, and K. Yang, "Wireless powered cooperation-assisted mobile edge computing," *IEEE Trans. Wireless Commun.*, vol. 17, no. 4, pp. 2375–2388, Apr. 2018.

[18] T. Q. Dinh, J. Tang, Q. D. La, and T. Q. S. Quek, "Offloading in mobile edge computing: Task allocation and computational frequency scaling," *IEEE Trans. Commun.*, vol. 65, no. 8, pp. 3571–3584, Aug. 2017.

[19] W. Wu *et al.*, "Robust secure beamforming for wireless powered full-duplex systems with self-energy recycling," *IEEE Trans. Veh. Technol.*, vol. 66, no. 11, pp. 10055–10069, Nov. 2017.

[20] Z. Chu, F. Zhou, Z. Zhu, M. Sun, and N. Al-Dhahir, "Energy beamforming design and user cooperation for wireless powered communication networks," *IEEE Wireless Commun. Lett.*, vol. 6, no. 6, pp. 750–753, Dec. 2017.

[21] Z. Chen, L. X. Cai, Y. Cheng, and H. Shan, "Sustainable cooperative communication in wireless powered networks with energy harvesting relay," *IEEE Trans. Wireless Commun.*, vol. 16, no. 12, pp. 8175–8189, Dec. 2017.

[22] P. Ramezani and A. Jamalipour, "Throughput maximization in dual-hop wireless powered communication networks," *IEEE Trans. Veh. Technol.*, vol. 66, no. 10, pp. 9304–9312, Oct. 2017.

[23] H. Chen, L. Xiao, D. Yang, T. Zhang, and L. Cuthbert, "User cooperation in wireless powered communication networks with a pricing mechanism," *IEEE Access*, vol. 5, pp. 16895–16903, 2017.

[24] W. Shin, M. Vaezi, J. Lee, and H. V. Poor, "Cooperative wireless powered communication networks with interference harvesting," *IEEE Trans. Veh. Technol.*, vol. 67, no. 4, pp. 3701–3705, Apr. 2018.

[25] L. Zhou, D. Wu, J. Chen, and Z. Dong, "When computation hugs intelligence: Content-aware data processing for industrial IoT," *IEEE Internet Things J.*, vol. 5, no. 3, pp. 1657–1666, Jun. 2018.

[26] L. Zhou, D. Wu, Z. Dong, and X. Li, "When collaboration hugs intelligence: Content delivery over ultra-dense networks," *IEEE Commun. Mag.*, vol. 55, no. 12, pp. 91–95, Dec. 2017.

[27] K. T. K. Cheung, S. Yang, and L. Hanzo, "Achieving maximum energy-efficiency in multi-relay OFDMA cellular networks: A fractional programming approach," *IEEE Trans. Commun.*, vol. 61, no. 7, pp. 2746–2757, Jul. 2013.

[28] H. Ju and R. Zhang, "Throughput maximization in wireless powered communication networks," *IEEE Trans. Wireless Commun.*, vol. 13, no. 1, pp. 418–428, Jan. 2014.

[29] L. Fan, R. Zhao, F. K. Gong, N. Yang, and G. Karagiannidis, "Secure multiple amplify-and-forward relaying over correlated fading channels," *IEEE Trans. Commun.*, vol. 65, no. 7, pp. 2811–2820, Jul. 2017.

[30] P. Ramezani and A. Jamalipour, "Fairness enhancement in dual-hop wireless powered communication networks," in *Proc. IEEE Int. Conf. Commun.*, 2017, pp. 1–6.

[31] M. Avriel, W. E. Diewert, S. Schaible, and I. Zang, *Generalized Concavity*. New York, NY, USA: Plenum Press, 1988.

[32] A. Zappone and E. Jorswieck, "Energy efficiency in wireless networks via fractional programming theory," *Found. Trends® Commun. Inf. Theory*, vol. 11, nos. 3–4, pp. 185–396, 2015.

[33] W. Dinkelbach, "On nonlinear fractional programming," *Manag. Sci.*, vol. 13, no. 7, pp. 492–498, 1967.

[34] S. Guo, B. Xiao, Y. Yang, and Y. Yang, "Energy-efficient dynamic offloading and resource scheduling in mobile cloud computing," in *Proc. IEEE Int. Conf. Comput. Commun. (INFOCOM)*, 2016, pp. 1–9.

[35] T. Soyata, R. Muraleedharan, C. Funai, M. Kwon, and W. Heinzelman, "Cloud-vision: Real-time face recognition using a mobile-cloudlet-cloud acceleration architecture," in *Proc. Comput. Commun.*, 2012, pp. 59–66.

[36] A. P. Miettinen and J. K. Nurminen, "Energy efficiency of mobile clients in cloud computing," in *Proc. USENIX Conf. Hot Topics Cloud Comput.*, 2010, p. 4.

[37] Y. Xiao, P. Savolainen, A. Karppanen, and M. Siekkinen, "Practical power modeling of data transmission over 802.11g for wireless applications," in *Proc. Int. Conf. Energy Efficient Comput. Netw.*, 2010, pp. 75–84.

[38] S. Boyd and L. Vandenberghe, *Convex Optimization*. Cambridge, U.K.: Cambridge Univ. Press, 2004.

Authors' photographs and biographies not available at the time of publication.